DEVELOPMENT OF PIV TECHNIQUE UNDER MAGNETIC FIELDS AND MEASUREMENT OF TURBULENT PIPE FLOW OF FLIBE SIMULANT FLUID

J. Takeuchi[1], S. Satake[2], T. Kunugi[3], T. Yokomine[4], N. B. Morley[1], M. A. Abdou[1]

[1]*University of California, Los Angeles, 420 Westwood Plaza, 44-114 Eng. IV, Los Angeles, CA 90095, USA*
takeuchi@fusion.ucla.edu
[2]*Tokyo University of Science, 2641 Yamazaki, Noda, Chiba 278-8510 Japan*
[3]*Kyoto University, Yoshida, Sakyo, Kyoto, 606-8501 Japan*
[4]*Kyushu University, 6-1 Kasuga-koen, Kasuga, Fukuoka 816-8580, Japan*

An investigation of MHD effects on a Flibe (Li_2BeF_4) simulant fluid has been conducted under the US-Japan JUPITER-II collaboration program using "FLIHY" pipe flow facility at UCLA. The present paper reports a development of unique experimental techniques using aqueous solution of potassium hydroxide as a Flibe simulant. In order to apply a particle image velocimetry (PIV) technique for magnetic field condition, special optical devices were developed. The PIV measurements of MHD turbulent pipe flow at Re = 5300 were performed, and modification of the mean flow velocity as well as turbulence suppression was observed. A flat velocity profile in the pipe center and a steep velocity gradient in the near-wall region at Ha = 20 exhibits typical characteristics of Hartmann flow.

I. INTRODUCTION

The design of tritium breeding blankets and plasma facing components is an important field in the R&D activities toward a viable commercial nuclear fusion reactor.[1] The main functions of the blankets for D-T fusion reactors are to breed tritium, to convert the kinetic energy of neutrons and X-rays into heat, and to provide radiation shielding. An essential idea of a liquid breeder concept is that if a liquid containing lithium can be introduced into the blanket, it can be used as both coolant and breeding material. In recent research, a molten salt coolant, Flibe, has attracted attention. Moriyama et al[2] surveyed various design concepts using Flibe and suggested its use in reactor designs where high temperature stability and low MHD pressure drop were special concerns. Among the design concepts utilizing Flibe are HYLIFE-II,[3] the APEX thick/thin liquid walls,[1] FFHR,[4] and a solid first wall design based on advanced nano-composited ferritic steel.[5]

Although Flibe has attractive features as coolant and tritium breeding material, there are some issues making Flibe-based blanket design challenging.[5] The main issues include 1) thermal conductivity of Flibe (1W/mK) is low compared to other lithium-containing metal alloys, Pb-17Li (15W/mK) and Li (50W/mK), 2) kinematic viscosity of Flibe is high, especially at temperatures close to the melting point (11.5mm^2/s at 500°C), and 3) the high melting point of Flibe requires structural material with temperature range over 650°C. The high viscosity and low thermal conductivity put Flibe in the class of high Prandtl number fluids. The limited temperature window above the high melting point of Flibe requires good heat transfer (low film temperature drop) to cool first wall structures. In order to obtain sufficiently large heat transfer using high Prandtl number fluid coolant, high turbulence is required. On the other hand, Wong et al[5] suggested that the parameter *Ha/Re* would exceed the critical value of 0.008, especially in large channels, which indicated the suppression of turbulence might be significant.[6] In this paper, Reynolds number is defined as $Re = U_bD/\nu$, and Hartmann number as $Ha = BR(\sigma/\rho\nu)^{1/2}$ where U_b, D, n, B, R, s and m are mean velocity, pipe diameter, kinematic viscosity, magnetic flux density, pipe radius, electrical conductivity and fluid density, respectively.

The MHD effects on turbulent flows have been investigated by many researchers; however, most of the experimental efforts were conducted using liquid metals as working fluids.[7,8] Liquid metals are generally classified as low Prandtl number fluids, and the heat transfer characteristics of low Prandtl number fluids are conduction dominant. Thus it is important to investigate the effect of magnetic fields on the turbulent flow and heat transfer characteristics of the high Prandtl number fluids.

To understand the underlying science and phenomena of fluid mechanics and heat transfer of Flibe, a series of experiments as a part of the US-Japan JUPITER-II collaboration are in progress. The approach includes flow and heat transfer measurements using a Flibe simulant fluid along with numerical simulation[9] and modeling.[10] A flow facility utilizing water and aqueous electrolytes as Flibe simulants has been constructed. Turbulent flow field measurements using PIV[11] and heat transfer

measurements[12] have been carried out without magnetic field to establish the experimental techniques and verify the performance of the facility by comparing an existing experimental result[13] and DNS data.[14]

The objectives of the present report are to describe the development of the experimental techniques under magnetic fields and introducing some preliminary results of the flow field measurements. In particular, the application of the PIV technique under difficult experimental conditions inside a narrow gap of the magnet is presented. Since most of the existing experimental data of MHD turbulent flows were obtained with liquid metals, flow visualization was impossible. The present work provides unique 2-dimensional 2-velocity-component information of the flow field to improve understandings of the MHD turbulent flows.

II. DEVELOPMENT OF EXPERIMENTAL TECHNIQUES

An experimental MHD flow facility called "FLIHY" (Flibe Hydrodynamics) has been constructed at UCLA. The facility consists of a flow loop with a pipe flow test section and integrated transparent visualization section, a magnet system, and a PIV measurement system. A 30% aqueous solution of potassium hydroxide (KOH hereafter) is used as the electrically conducting working fluid.

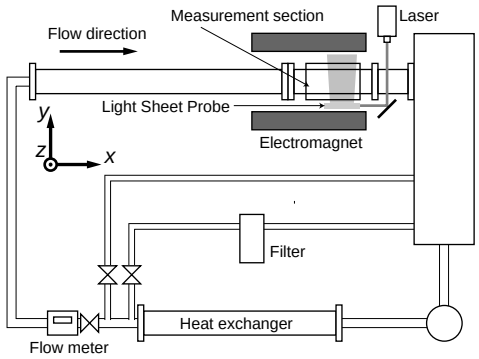

Fig. 1. Schematic drawing of pipe flow facility

II.A. Flow Facility

A schematic drawing of the pipe flow apparatus is shown in Fig. 1. The fluid flow is circulated by a pump and introduced into the horizontal circular pipe test section. Flow passes through a heat exchanger, a flow meter, and a honey comb flow straightener before entering the test section. The temperature of the fluid is monitored by T-type thermocouples and controlled using the heat exchanger flow. The test section is a circular pipe made of acrylic with 89 mm inner diameter and 7.0 m in length, which is 79 times the pipe diameter. This length is considered to be sufficient to obtain a fully developed turbulent flow. This relatively large diameter was chosen to allow access to information in near-wall region by making viscous length scale large. Flow rate is controlled by changing the pump output with a variable frequency power controller. A throttle valve in the main loop and a bypass line are also equipped to help flow rate control. The flow rate is measured and monitored by vortex-shedding type flow meter.[15]

The visualization section for the PIV measurement was built 6.8 m downstream from the inlet. The pipe wall thickness in the visualization section is 1 mm to allow velocity measurement down to very close to the pipe wall. A "water jacket" tank with square cross section was installed surrounding the pipe. The cross section view of the water jacket is shown in Fig. 2. The water jacket is 11 × 11 cm in the cross section and 23 cm long. It was filled with the same fluid as the main flow in order to compensate for the image distortion due to the difference in index of refraction between inside and outside of the circular pipe. This eliminates the optical distortion to a negligible level.

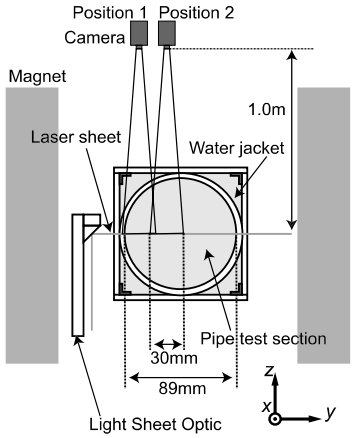

Fig. 2. Cross section view of water jacket and optical configuration

II.B. Magnet

The magnet used for the current experiments produces maximum 2.0 Tesla magnetic fields in a narrow gap of the iron core at 3000 A of applied electric current. The pipe flow test section was placed in the gap which is 1.4 m in the streamwise direction, 25 cm in height, and 15 cm in width. The B field distribution at the center of the streamwise cross section as a function of the distance from the magnet center is shown in Fig. 3. The B field has uniform distribution within 5% variation for 1.0 m in the streamwise direction. Fig. 3 also shows the B field distribution in the center cross section in the streamwise direction. There is no direct proof showing the flow development length under the magnetic field is sufficient to fully establish the MHD effects; however, the 13 diameter development length is considered to be sufficient at Re = 5300 because DNS[15] simulations suggests

approximately 9 diameters is sufficient, and Joule time scale $\tau_j = \rho/\sigma B^2$ gives similar result.

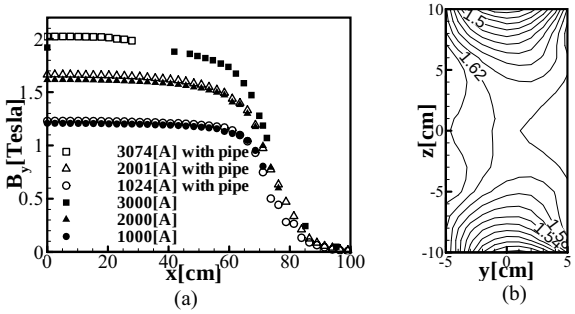

(a) (b)

Fig. 3. B field distributions (a) as function of the streamwise distance from the magnet center and (b) at the center cross section at 2000 A

II.C. PIV SYSTEM

The PIV technique has been developed in last two decades and has become a well established technique for flow field measurements.[17] However, there were some difficulties in application under the magnetic fields due to the limited space in the magnet gap and the limited types of the material that can be used under the strong magnetic fields condition with a corrosive working fluid. Therefore, the PIV system specifically tailored for the current experiment was developed by carefully selecting the materials and optical component placement to cope with these difficulties.

II.C.1. Seeding Particles

Seeding particles were selected so that they are compatible with KOH and their density was comparable to that of KOH (1300 kg/m^3). Methyl methacrylate – ethylene glycol dimethacylate copolymer (Sekisui Plastic Co., Ltd.) turned out to be compatible as well as to have the density close to the solution (about 1200 kg/m^3). Although it was not specifically tailored for PIV use, its relatively uniform particle diameter (5μm) was suitable for PIV measurements.

II.C.2. PIV Hardware

A laser beam supplied by New Wave Solo-III Nd:YAG Laser is introduced into the magnet gap using a dielectric coated mirror. Light sheet optic (Fig. 4) placed in the magnet gap converts the laser beam into a thin sheet less than 1 mm in thickness with a cylindrical lens and introduces it horizontally to the measurement plane with two dielectric mirrors.

The particle images illuminated by the laser sheet are captured by Phantom v.5.0 high speed camera (Vision Research Inc.). The camera has 1024×1024 pixels monochrome CMOS array. Tamron SP 35-210 mm lens is used along with extension tubes to achieve 90×90 and 30×30 mm field of view on the measurement plane 1.0 m from the lens.

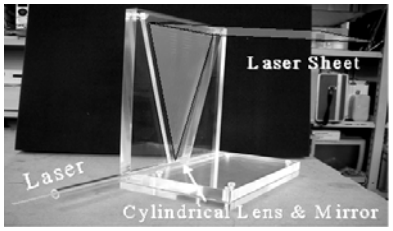

Fig. 4. Light sheet optic

Synchronization of the laser shootings and the camera exposures are controlled by LabSmith LC880 experiment controller. The camera strobe signal is used as a master trigger signal, and the laser firings are controlled by setting delay times from the master signal for flash lamps (F) and Q-switches (Q) for each laser rod as shown in Fig. 5.

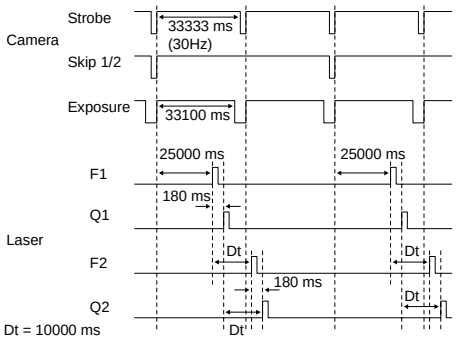

Fig. 5. Synchronization chart

II.C.3. PIV Analysis Software

Dantec FlowManager 3.70 software is used for PIV analysis. It provides analysis method called "adaptive correlation", which is based on commonly used cross correlation technique.[18] The important feature of the adaptive correlation is a multiple step analysis method.[19] Large interrogation windows are used in the first step and the interrogation windows are successively reduced in the following steps. For this experiment, the reduction of the window size is repeated 4 times. Thus 256 × 128 pixels interrogation windows in the first step are reduced to 32 × 16 pixels in the final step. In each step, cross correlation analysis is performed twice. The first analysis gives a rough estimate of the particle displacement by analyzing exactly the same area in the first and second images, and the location of the interrogation windows in the second analysis is determined using the information given by the first analysis in order to minimize loss of particle pairs in the windows.[20] To reduce the possibility of yielding spurious vectors due to mismatch of the particle pairs, local median validation is applied between the steps, and

the invalidated vectors are replaced by using information from the vectors in vicinity.[21] The particle displacement was determined down to sup-pixel order. A Dantec 80S33 high accuracy software module is used for this experiment. This module has an advantage over the conventional three-point Gaussian curve fitting method; however, access to the detail of the algorism is prevented by proprietary information issue.

II.D. PROPERTIES OF KOH SOLUTION

In order to determine some of the more critical thermo-physical properties of 30% KOH aqueous solution, measurements were carried out. The kinematic viscosity was measured by U-tube capillary viscometer. The electrical conductivity was measured by conductivity meter. Other properties were quoted from the reference book.[22] TABLE I shows the thermo-physical properties at 33.8°C experimental temperature.

TABLE I. Properties of KOH solution at 33.8°C

ρ	Density	1280 [kg/m^3]
μ	Viscosity	1.431×10^{-3} [Pa·s]
ν	Kinematic viscosity	1.118×10^{-6} [m^2/s]
σ	Electrical conductivity	73.67 [S/m]
λ	Heat conductivity	0.727 [W/(m·K)]
Cp	Heat capacity	3.00 [J/(kg·K)]
Pr	Prandtl number	5.90

III.MHD TURBULENT FLOW MEASUREMENTS

III.A. Experimental Procedures

Experiments were performed by the following procedures. A calibration target was inserted in the test pipe. The camera placement was adjusted so that the field of view encompassed the pipe diameter. The camera focus was focused on the calibration plate at the bisection plane, and calibration images were taken. The correspondence of the pixel length to the physical length was determined by reading the pixel numbers and the physical position of the calibration image on the computer monitor. After the calibration target was removed, flow rate was adjusted to 25 liters per minute, which corresponds to Re = 5300.

The mean velocity measurements were performed for five different Hartmann numbers, Ha = 0, 5, 10, 15, 20. 2000 images were taken for each Hartmann number, and the mean velocity profiles were calculated by ensemble averages of 1000 instantaneous velocity vectors and streamwise average of 127 vectors.

III.B. Results

Instantaneous fluctuating velocity vector maps are shown in Fig. 6 with various Hartmann numbers. The fluctuating velocity field at (a) Ha = 0 shows commonly observed near-wall turbulence structure. By increasing Hartmann number, the turbulence fluctuations decrease and the near-wall structures disappear.

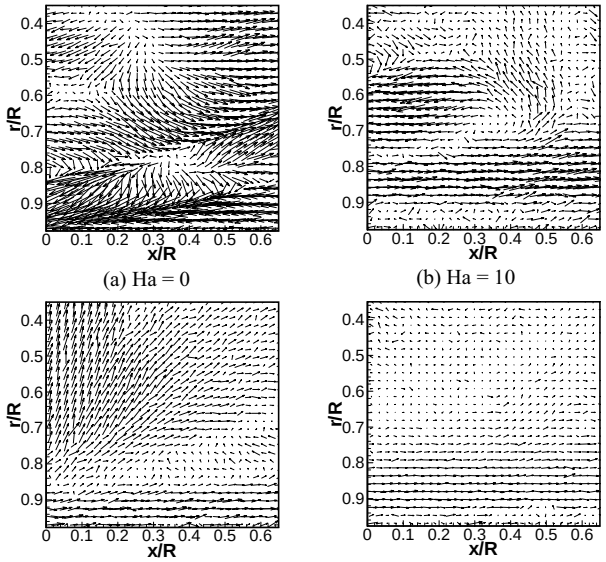

(a) Ha = 0 (b) Ha = 10

(c) Ha = 15 (d) Ha = 20

Fig. 6. Fluctuating velocity vector maps with variable Hartmann number

The mean velocity distributions at Re = 5300 normalized by centerline velocity with variable Hartmann number are shown in Fig. 7. The centerline velocities for each Hartmann numbers are tabulated in TABLE II. The mean velocity profiles show that they become flatter as Hartmann number increases in the core region and that the near-wall velocity gradient increases with increasing Hartmann number, showing typical characteristics of Hartmann flow.[7]

TABLE II. Centerline velocities with variable Ha

Ha	0	5	10	15	20
U_c [$\times 10^{-2}$ m/s]	8.86	8.84	8.71	8.49	8.41

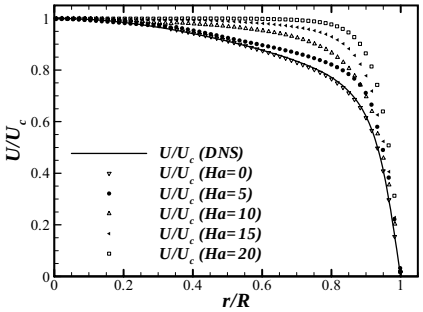

Fig. 7. Mean velocity distritution at Re = 5300

IV.CONCLUSIONS

The PIV measurement technique for MHD turbulent flow of Flibe simulant fluid has been developed. The

major difficulties arisen from the limited space in the gap of the magnet and material limitation due to the strong magnetic field were overcome by specially tailored optical components. The measurement of the MHD turbulent pipe flow yielded unique 2-D 2-component vector maps showing the modification of the mean flow and the suppression of turbulence by MHD effects. Additional experiments are underway to quantify the effect of MHD on fluctuating turbulent velocity components and their subsequent effect on turbulent heat transfer for fusion blankets.

ACKNOWLEDGMENTS

Authors are grateful for the financial support from the U.S. D.O.E., Grant No. DE-FG03-86ER52123, and the Japanese Ministry of Education, Culture, Sports, Science and Technology via the JUPITER-II collaboration.

REFERENCES

1. M. A. ABDOU, THE APEX TEAM and A. YING et al., “On the Exploration of Innovative Concepts for Fusion Chamber Technology,” *Fusion Eng Des*, **54**, 181 (2001)
2. H. MORIYAMA, A. SAGARA and S. TANAKA et al, "Molten Salts in Fusion Nuclear Technology," *Fusion Eng. Des.*, **39-40**, 627, (1998).
3. R. W. MOIR, R. L. BIERI and X. M. CHEN et al, "HYLIFE-II: A molten-salt inertial fusion energy power plant design - final report," *Fusion Technol.*, **25**, 5, (1994).
4. A. SAGARA, H. YAMANISHI and S. IMAGAWA et al, "Design and Development of the Flibe Blanket for Helical-Type Fusion Reactor FFHR," *Fusion Eng. Des.*, **49-50**, 661, (2000).
5. C. P. C. WONG, S. MALANG and M. SAWAN et al, "Molten Salt Self-Cooled Solid First Wall and Blanket Design Based on Advanced Ferritic Steel," *Fusion Eng. Des.*, **72**, 245, (2004).
6. E. BLUMS, YU. A. MIKHAILOV and R. OZOLS, *Heat and Mass Transfer in MHD Flows*, World Scientific, Singapore, (1987).
7. R. A. GARDNER and P. S. LYKOUDIS, "Magneto-Fluid Mechanic Pipe Flow in A Transverse Magnetic Field. Part 1. Isothermal Flow," *J. Fluid Mech.*, **47**, 737, (1971).
8. C. B. REED and P. S. LYKOUDIS, "The Effect of a Transverse Magnetic Field on Shear Turbulence," *J. Fluid Mech.*, **89**, 147, (1978).
9. S. SATAKE, T. KUNUGI and S. SMOLENTSEV, "Direct Numerical Simulations of Turbulent Pipe Flow in a Transverse Magnetic Field," *J. Turbulence*, **3**, 020, (2002).
10. S. SMOLENTSEV, M. A. ABDOU and N. B. MORLEY et al, "Application of the K-ε model to open channel flows in a magnetic field," *Int. J. Eng. Sci.*, **40**, 693, (2002).
11. J. TAKEUCHI, S. SATAKE and N. B. MORLEY et al, "PIV Measurements of Turbulence Statistics and Near-Wall Structure of Fully Developed Pipe Flow at High Reynolds Number," *Proc. 6th International Symposium on Particle Image Velocimetry*, Pasadena, CA, USA, Sept 21-23, (2005).
12. J. TAKEUCHI, S. SATAKE and R. MIRAGHAIE et al, "Study of Heat Transfer Enhancement / Suppression for Molten Salt Flows in a Large Diameter Circular Pipe: Part One - Benchmarking," *Fusion Eng Design*, 81, 601, (2006).
13. J. G. M. EGGELS, F. UNGER and J. WEISS et al, "Fully Developed Turbulent Pipe Flow: A Comparison between Direct Numerical Simulation and Experiment," *J. Fluid Mech.*, **268**, 175, (1994).
14. S. SATAKE, T. KUNUGI and R. HIMENO, "High Reynolds Number Computation for Turbulent Heat Transfer in Pipe Flow,” In: M. Valero et al, Ed., *Lecture Notes in Computer Science 1940*, Springer-Verlag, Berlin-Heidelberg, (2000).
15. S. Satake, Private communication, (2004).
16. R. J. GOLDSTEIN, *Fluid Mechanics Measurements*, Hemisphere Publishing, (1987), pp. 262
17. M. RAFFEL, C. E. WILLERT and J. KOMPENHANS, *Particle Image Velocimetry: A Practical Guide*, Springer-Verlag, Berlin-Heidelberg, (1998).
18. R. D. KEANE and R. J. ADRIAN, "Theory of Cross-Correlation Analysis of PIV Image,” In: F. M. T. Nieuwstadt Ed., *Flow Visualization and Image Analysis*, Kluwer Academic Publishers, Netherlands, (1993).
19. F. SCARANO and M. L. RIETHMULLER, "Iterative Multigrid Approach in PIV Image Processing with Discrete Window Offset," *Exp. Fluids*, **26**, 513, (1999).
20. J. WESTERWEEL, D. DABIRI and M. GHARIB, "The Effect of a Discrete Window Offset on the Accuracy of Cross-Correlation Analysis pf Digital PIV Recordings," *Exp. Fluids*, **23**, 20, (1997).
21. J. WESTERWEEL, "Efficient Detection of Spurious Vectors in Particle Image Velocimetry Data," *Exp. Fluids*, **16**, 236, (1994).
22. A. L. HORVATH, *Handbook of Aqueous Electrolyte solutions*, Ellis Horwood, Chichester, (1985).